Communications

Reduction of Motion Artifacts Using a Two-Frequency Impedance Plethysmograph and Adaptive Filtering

Javier Rosell, Kevin P. Cohen, and John G. Webster

Abstract— **We measured transthoracic impedance in nine presumed healthy adult subjects with a two-frequency plethysmograph at 57 kHz and 185 kHz. The measurement protocol included periods of normal breathing without motion and periods of motion without breathing. We analyzed the cross-correlation and the ratio between the signals at both frequencies for all the different maneuvers. The correlation coefficient was between 0.97 and 1 for breathing, the minimal cross-correlation (0.81) was for simulated obstructive apnea. We found that the amplitude ratio between the two-frequency signals was different for normal breathing and for motion. Based on these results, we designed and tested an adaptive filter to increase the signal-to-artifact ratio (SAR). The increase in SAR (mean ± standard deviation) compared with the signal at 57 kHz was: 183% ± 117% for arm movement, 133% ± 93% for leg movement, and 34% ± 62% for simulated obstructive apnea.**

I. Introduction

Impedance plethysmography is a well known and extensively used noninvasive method for ventilation and apnea monitoring [1]. The method consists of injecting a low-amplitude high-frequency current through the ribcage with two electrodes. Air volume variation in the lungs and variations of the ribcage shape modifies the electrical impedance, modulating the voltage drop across the body. The voltage is then measured with the same pair of electrodes (bipolar or two-electrode method) or with another pair (tetrapolar method) [2]. After amplification and filtering, the impedance changes are detected by amplitude demodulation.

A major problem with this technique is its sensitivity to body movement [3]–[5]. Changes in the ribcage shape and/or in the skin-to-electrode impedance can produce large amplitude artifacts, in many cases larger than the breathing-related signal. Also, in neonates and infants, the impedance fluctuations caused by cardiac activity could be misclassified as breathing, which could falsely prevent an alarm during apnea [3]. To increase the signal-to-artifact ratio (SAR) two alternatives have been studied. The use of different electrode configurations [6] is intended to reduce the effect of variations in the skin-to-electrode contact impedance but fails to reduce the effect of ribcage-shape changes unrelated to breathing. The use of different electrode location [7] tries to minimize the effect of movements but the results show that the best location is patient dependent.

Another approach to reduce motion artifacts is to use multiple sensors containing independent information about breathing and motion. Cohen *et al.* [8] used inductive belt and impedance techniques simultaneously in the thorax and ribcage to distinguish between motion and ventilation. Also, using two inductive belts on the ribcage and abdomen and an adaptive filter, East *et al.* [9] were able to detect patient motion unrelated to breathing. Based on this approach, and trying to maintain the simplicity of impedance measurements, we decided to measure at different frequencies and combine the signals to increase the SAR.

Our initial hypothesis was that components of the impedance signal related to actual changes of air volume in the lung and to nonventilatory movements would have different amplitudes at different carrier frequencies. To assess this hypothesis, a two-frequency impedance plethysmograph was used to measure ventilatory and nonventilatory movements. This paper summarizes the results and proposes a method based on an adaptive filter to detect and reduce motion artifacts.

II. Data Acquisition

We used a custom two-channel impedance plethysmograph. Each channel was able to work between 10 kHz and 200 kHz. We tried different pairs of frequencies, but in this paper we will only analyze the results using 57 and 185 kHz. We selected these frequencies taking into account the following factors: 1) maximize the difference between low and high frequency, 2) the high frequency must be centered between harmonics of the low frequency to avoid intermodulation, 3) our system specifications, and 4) minimize the skin-to-electrode impedance. We noticed that the cross-correlation was lower for frequencies below 50 kHz and this could be due to the increase in skin-to-electrode impedance below this frequency [10], a larger contact impedance induces problems of dynamic range, and more electrode-related artifacts.

We used a two-electrode method with the current sources and the voltage inputs of both channels connected in parallel to the same electrodes. Total current injected was 0.1 mA_{rms}. The equipment used analog multipliers to detect the in-phase component in each channel. Measured phase errors were less than 1 degree at both frequencies. The outputs of the demodulators were ac-coupled and amplified. Both channels had a high-pass filter at 0.03 Hz and a low-pass filter at 10 Hz (−3 dB).

We measured nine subjects (ages 22–44) with no known respiratory abnormalities. Two Ag/AgCl electrodes (Signa II, Burdick Corp.) were placed at opposite midaxillary lines one centimeter under the nipples. The volunteers were asked to rest in a quiet supine position and then perform the following maneuvers: 1) 10 s without breathing, 2) 20 s normal breathing, 3) raising and lowering the arms without breathing for 15 s, 4) ribcage breathing for 30 s, 5) raising and lowering the legs without breathing for 15 s, 6) abdominal breathing for 30 s, and 7) to simulate an obstructive apnea moving air from the ribcage to the abdomen and back again without breathing for 15 s. A detailed description of the protocol and the results, at frequencies between 12.5 kHz and 185 kHz, is in [11].

Both channels were sampled at 50 Hz with a 16-b A/D card (National instruments NB-MIO-16H). Data were stored using Labview for further analysis with MatLab.

III. Data Analysis

To determine the relation between the information acquired at each frequency, we calculated the cross-correlation coefficient between the 57 and 185 kHz signals for each maneuver. When the cross-

Manuscript received July 5, 1994; revised April 6, 1995. The work of J. Rosell, as a Visiting Professor at the University of Wisconsin-Madison, was supported by the Spanish DGICYT Grants 93-197 and PB92/0892. The work of K. P. Cohen was supported by a graduate fellowship in biomedical engineering from the Whitaker Foundation.

J. Rosell is with the Departament d'Enginyeria Electrònica, Universitat Politècnica de Catalunya, 08071 Barcelona, Spain.

K. P. Cohen and J. G. Webster are with the Department of Electrical and Computer Engineering, University of Wisconsin, Madison, WI 53706 USA.

IEEE Log Number 9414169.

TABLE I
MEAN AND MINIMUM CROSS-CORRELATION COEFFICIENT FOR NORMAL BREATHING AND DIFFERENT MANEUVERS

MANEUVER	Crosscorrelation coefficient	
	Mean	Minimum
Normal breathing	0.994	0.97
Arm movement	0.986	0.97
Leg movement	0.991	0.97
Sim. obstructive apnea	0.960	0.81

correlation was high, we also made a linear regression between channels to determine the amplitude ratio. Based on these results, we proposed a mathematical model to explain how the adaptive filter works.

A. Cross-Correlation Coefficients

We defined windows of 15 s during each maneuver and calculated the cross-correlation coefficient between both channels for each maneuver and subject. Table I shows the mean and lowest cross-correlation coefficients for each maneuver in our sample. The values are very close to one, indicating that the signal source is the same at both frequencies. For simulated obstructive apnea, we obtained the lowest cross-correlation. A possible explanation is that the signal is smaller and uncorrelated noise becomes more significant.

As the cross-correlation coefficient is normalized by the powers of both input signals, it does not give information about the relative amplitudes of this signals. In the next section, we analyze the amplitude ratio between the high-frequency (x_{HF}) and the low-frequency (x_{LF}) signals.

B. Ratio HF/LF

We selected the same 15-s intervals used in the cross-correlation analysis for each maneuver and calculated the ratio between both signals (R_{HL}) as the slope of a linear least square fit

$$x_{\mathrm{HF}}(t) = R_{\mathrm{HL}} x_{\mathrm{LF}}(t) + b. \tag{1}$$

Table II shows the mean and standard deviation for the ratio (R_{HL}). The group of maneuvers that produces actual ventilation—normal, ribcage, and abdominal breathing—have similar results with the mean values differing only by 0.02, that is almost half its standard deviation. It is also important to note the small variation between subjects for this ratio, in contrast with the large variations of amplitude between subjects at a given frequency at the same ventilation level [4].

R_{HL} for arm and leg movement is significantly different from R_{HL} during maneuvers that produce ventilation (a t-test gave significant levels of 0.002 and 0.005, respectively). For motion, the variability in the ratio is larger, especially for simulated obstructive apnea. The increase in the standard deviation for this maneuver could be explained by anatomical differences and differences in the movements and the intensity in which every subject tried to simulate obstructive apnea.

C. Model

Based on these results, we could decompose the signals at high and low frequency into three components: signal related to ventilation $s(t)$, signal related to artifacts (or other correlated noise) $n_c(t)$, and uncorrelated noise $n_1(t)$ and $n_2(t)$

$$x_{\mathrm{HF}}(t) = A_1 s(t) + B_1 n_c(t) + n_1(t) \tag{2}$$

$$x_{\mathrm{LF}}(t) = A_2 s(t) + B_2 n_c(t) + n_2(t) \tag{3}$$

TABLE II
MEAN RATIO $R_{\mathrm{HL}} \pm$ STANDARD DEVIATION BETWEEN THE SIGNAL AT 185 KHZ AND THE SIGNAL AT 57 KHZ, FOR DIFFERENT TYPES OF BREATHING AND MOTION WITHOUT BREATHING

Ventilation			Motion artifact		
Normal	Ribcage	Abdom.	Arms	Legs	Obstr.
1.11 ±0.04	1.09 ±0.04	1.10 ±0.06	0.84 ±0.10	0.95 ±0.08	1.21 ±0.16

where A_1, A_2, B_1, and B_2 are the gains for the signals and artifacts at each frequency. If we assume that all the signals have zero mean, these gains are related to R_{HL}, defined in (1), by

$$R_{\mathrm{HL}}(\text{ventilation}) = \frac{A_1}{A_2}$$

and

$$R_{\mathrm{HL}}(\text{motion}) = \frac{B_1}{B_2}. \tag{4}$$

Thus, Table II could be used to determine these gain ratios.

According to this model, it is theoretically possible to cancel the effect of motion artifacts using a linear combination of $x_{\mathrm{HF}}(t)$ and $x_{\mathrm{LF}}(t)$

$$y(t) = \frac{B_2}{B_1} x_{\mathrm{HF}}(t) - x_{\mathrm{LF}}(t) \tag{5}$$

$$y(t) = \left(\frac{B_2}{B_1} A_1 - A_2\right) s(t) + \frac{B_2}{B_1} n_1(t) - n_2(t). \tag{6}$$

The output $y(t)$ will be related to ventilation only if the ratios A_2/A_1 and B_2/B_1 are not equal.

To assess the assumption implicit in the model that if ventilation and motion are simultaneously present then the output signal is the linear addition of both, we measured two subjects with intervals of breathing only, movement only, and simultaneous breathing and movement. We instructed the subjects to perform the same limb movements with or without breathing. A pneumotachometer was also used as a standard to measure the ventilation. We calculated R_{HL} for maneuvers with breathing without motion and motion without breathing. When only motion was present, R_{HL} is equal by definition to B_1/B_2. When both were present, we calculated the optimal weight for $x_{\mathrm{LF}}(t)$ to minimize the quadratic error between the pneumotachometer and the sum of both signals. According to (5), to cancel the effect of motion artifacts this weight must be equal to B_2/B_1. In our measurements for both subjects, the optimal weight to minimize the error was within the range of $B_2/B_1 \pm 10\%$.

Differences in the ratio B_2/B_1 for diverse types of movement and different subjects implies that we have to dynamically change the weights in (5) to cancel the motion artifacts. We propose to use an adaptive filter to enhance the signal, reducing artifacts, and correlated noise [12].

IV. ADAPTIVE FILTER

To cancel noise using an adaptive filter, we need a reference signal containing only correlated noise with the primary input [12], [13]. In our case, we could obtain this reference as follows:

$$y_1(t) = \frac{A_2}{A_1} x_{\mathrm{HF}}(t) - x_{\mathrm{LF}}(t) \tag{7}$$

$$y_1(t) = \left(\frac{A_2}{A_1} B_1 - B_2\right) n_c(t) + \frac{A_2}{A_1} n_1(t) - n_2(t). \tag{8}$$

$y_1(t)$ will be the reference signal for the adaptive filter as shown in Fig. 1. To reduce uncorrelated noise with averaging, we used as the primary signal the sum of $x_{\mathrm{HF}}(t)$ and $x_{\mathrm{LF}}(t)$.

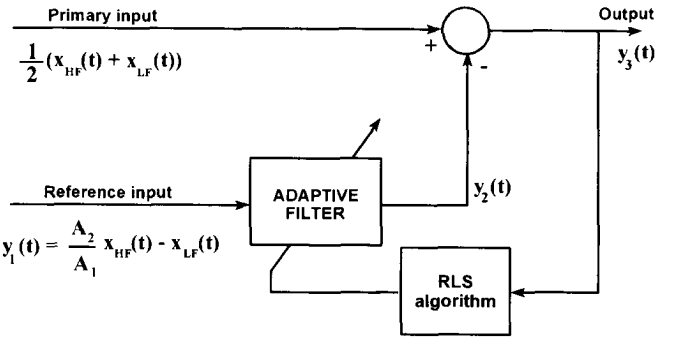

Fig. 1. The adaptive filter uses R_{HL}, the ratio of ventilation signals, and an RLS algorithm to cancel motion artifacts.

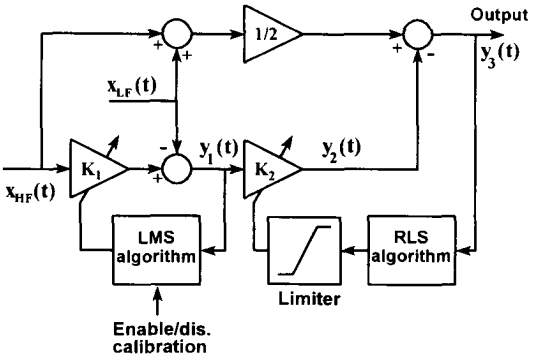

Fig. 2. The final implementation uses K_1, the adjusted ratio R_{HL}, for the adaptive filter. The enable/disable calibration input is used to adjust K_1 during normal breathing.

As the reference signal and the noise present in the primary input only differ in amplitude, we used an adaptive filter of order zero. If the power of uncorrelated noise is smaller than the power of the correlated signal, after adaptation the value for the gain is

$$K_2 = \frac{1 + \frac{B_2}{B_1}}{2\left(\frac{A_2}{A_1} - \frac{B_2}{B_1}\right)} \tag{9}$$

and the output signal

$$y_3(t) = \frac{A_1 + A_2}{2} s(t) + n_1(t)\left[\frac{1}{2} - K_2 \frac{A_2}{A_1}\right] + n_2(t)[\tfrac{1}{2} + K_2]. \tag{10}$$

As an example, if only arm movement occurs during breathing and we take the mean values of Table II, we obtain

$$y_3(t) \cong s(t) - 3.4n_1(t) + 4n_2(t). \tag{11}$$

This example shows that uncorrelated noise increases when the filter is trying to cancel motion artifacts. In practice, the amplitude of artifacts is orders of magnitude larger than the uncorrelated noise and we will have an effective increase in signal-to-noise ratio. If there are no artifacts, the gain of the filter (K_2) will converge to an optimal value to reduce the effect of $n_1(t)$ and $n_2(t)$ because these signals are present in the primary and reference inputs and will be treated as correlated noise.

A practical problem is the variability in the ratio A_1/A_2 for different subjects and types of breathing. If the actual value differs from the one used, the reference signal will also contain a residual part of $s(t)$. If this is the case, the adaptive filter will cancel part of $s(t)$. In order to adjust the ratio A_2/A_1, to minimize $s(t)$ in the reference input, we used another adaptive filter. Fig. 2 shows the final implementation of our algorithm. The first adaptive loop is only active during a learning interval at the beginning of each acquisition during normal breathing. The value for K_1 after adaptation will be

$$K_1 = \frac{A_2}{A_1}. \tag{12}$$

For the first adaptive filter we used an LMS algorithm ($k = 0.003$) for its simplicity. For the second, we used an RLS algorithm to optimize the adaptation speed with a forgiveness factor of 0.997 [13]. For some registers, we increased the order of the filter up to eight, but the improvement of the output signal was not significant. This result shows that the model established in (1) and (2) is accurate in the sense that the artifact signal is correlated in both channels and there is only a gain difference with minimal phase shift.

Theoretically, if the signal-to-artifact ratio at the reference signal is SAR_{ref}, the signal-to-artifact ratio at the output after adaptation will be $1/SAR_{ref}$ [12]. To calculate the resulting SAR, we have to define the gain error (ε) in K_1 given by

$$K_1 = \frac{A_2}{A_1}(1 + \varepsilon) \tag{13}$$

and the distance (D) between breathing and motion artifact defined by

$$\frac{B_2}{B_1} = \frac{A_2}{A_1}(1 + D). \tag{14}$$

With these definitions, the SAR at the output will be

$$SAR_{OUT} = \left[\frac{\varepsilon - D}{\varepsilon}\right] \frac{1}{SAR_{HF}} \tag{15}$$

where SAR_{HF} is for the SAR for the high-frequency signal.

This result shows that the best improvement is obtained when the SAR at the inputs is smaller than 0 dB, or when the gain K_1 is accurate. In our experiment, during the maneuvers with artifacts there is no breathing, therefore the SAR_{HF} is zero and the theoretical filter output must be zero. A problem could arise for high SAR at the input. In this case, small errors in the adjustment of K_1 could reduce the SAR. To avoid this effect, we limited the range of the gains (K_2) in the adaptive filter to ± 10. With this limit, we could have an error up to 10% in K_1 and the output will still be proportional to $s(t)$ having only a gain error.

V. Results

To quantify the improvement introduced by the adaptive filter we used an equivalent signal-to-artifact ratio defined as the ratio between the rms value for normal breathing (maneuver #2) and the rms value for each motion artifact (maneuvers #3, #5, and #7) (note that this definition of SAR is not the same as used in the previous section where the signal and the artifact occur simultaneously). Table III shows the individual results for all the subjects at a single frequency and the improvement introduced by the adaptive filter. We defined the improvement as

$$IMP(\%) = 100\,\frac{SAR_{OUT} - SAR_{IN}}{SAR_{IN}} \tag{16}$$

where SAR_{IN} is the SAR for the 57- or 185-kHz signals and SAR_{OUT} is at the adaptive filter output.

For arm and leg movements, we obtained significant improvement on all but one subject. The mean improvement with respect to the signal at 57 kHz, which is a frequency close to the ones commonly used, is 183% for arm movement and 133% for leg movement. For simulated obstructive apnea, the results show a great subject variability with a mean improvement of only 34%.

TABLE III
SIGNAL-TO-ARTIFACT RATIO FOR ARM MOVEMENT, LEG MOVEMENT, AND SIMULATED OBSTRUCTIVE APNEA FOR ALL THE SUBJECTS AT BOTH FREQUENCIES (LF: 57 KHZ, HF: 185 KHZ). IMP(%) IS THE PERCENTAGE IMPROVEMENT BETWEEN THE ADAPTIVE FILTER OUTPUT AND THE SIGNALS AT LF AND HF

S#	SAR(%)			IMP(%)	
	LF	HF	OUT	LF->OUT	HF->OUT
ARM MOVEMENT					
1	10	16	29	189	81
2	93	115	400	328	248
3	53	71	96	83	36
4	58	82	137	134	67
5	25	30	56	126	88
6	10	12	51	413	313
7	46	55	52	12	-6
8	182	244	435	139	78
9	7	7	21	220	181
			Mean	183	121
			STD	117	98
LEG MOVEMENT					
1	35	46	154	337	235
2	101	125	250	148	100
3	71	88	152	112	73
4	65	70	161	148	129
5	47	58	120	154	108
6	50	61	141	182	131
7	213	244	208	-2	-15
8	270	323	556	106	72
9	19	20	22	14	8
			Mean	133	94
			STD	93	69
OBSTRUCTIVE					
1	256	204	167	-35	-18
2	769	833	909	18	9
3	192	238	250	30	5
4	204	149	250	23	68
5	270	263	208	-23	-21
6	156	213	238	52	12
7	103	109	303	194	178
8	313	238	385	23	62
9	24	25	29	21	19
			Mean	34	35
			STD	62	58

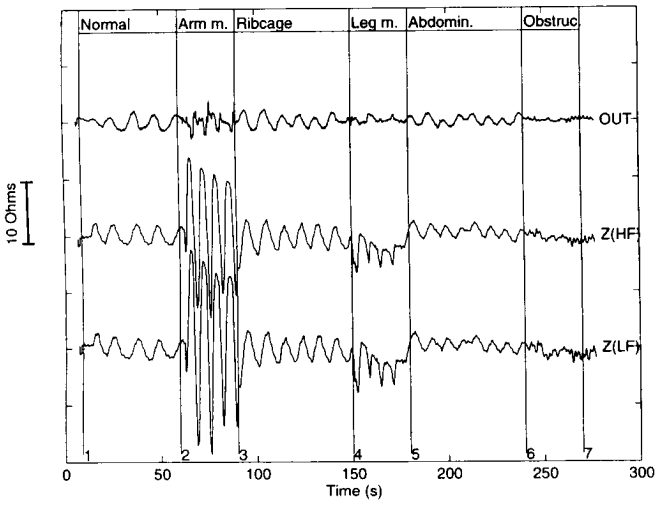

(a)

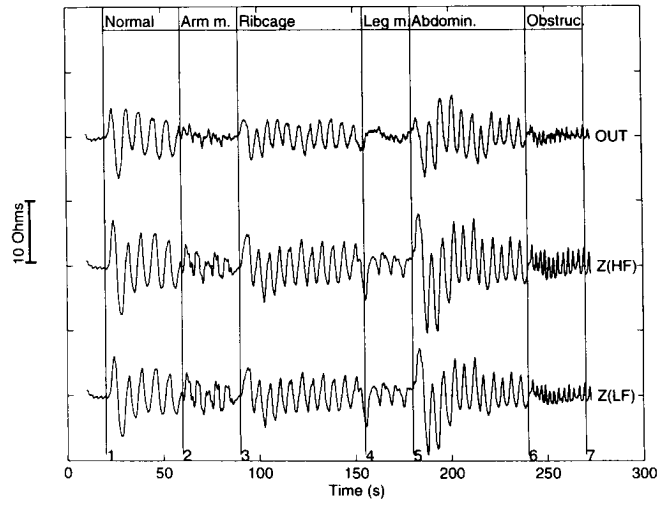

(b)

Fig. 3. Results for two representative subjects: (a) poor subject #6, and (b) best subject #8. Note arm and leg motion artifact Z_{HF} and Z_{LF} reduced at OUT.

Fig. 3 shows the results for two representative subjects, subject #6 has one of the poorest SAR's and subject #8 one of the best SAR's. The two lower traces show the signals at 185 kHz [Z(HF)] and 57 kHz [Z(LF)] and the upper trace shows the adaptive filter output (OUT). It is clear that we obtain a reduction of the amplitude of motion artifacts at the output of the filter compared to the single-frequency signals.

In Fig. 3(a), subject #6 shows for arm movement a very poor SAR of 10% and 12% at 57 and 185 kHz respectively (Table III). After the filter, the SAR is 51%, but also the signal waveform differs substantially from a typical breath, having more high-frequency components. For all subjects, we found that this shift to high frequency could be used to further distinguish artifact from breathing.

Cardiac artifact is a problem when monitoring neonates and infants, and sometimes apnea monitors could misclassify cardiac artifact as breathing [3], [14]. In our measurements in adults, we obtained an R_{HL} of 0.9 for the cardiac-related signal that could be distinguished from breathing with an R_{HL} of 1.10. However, in this experiment, it was not possible to show the reduction of cardiac artifacts due to the low level that this artifact has in adults.

VI. CONCLUSIONS

The differences in ventilation and motion artifacts at different frequencies could be used to detect and reduce motion artifacts. With a two-frequency impedance plethysmograph and the use of an adaptive filter, we obtained a mean increase of SAR of 182% for arm movement and 133% for leg movement compared with a 57 kHz signal. The improvement for simulated obstructive apnea was smaller (34%) with a larger subject-to-subject dispersion (62%). A main advantage of this method is that it requires no additional electrodes or connectors and could be implemented easily.

The SAR at the output is basically proportional to the inverse of the SAR at one single frequency. Therefore, the best improvement in SAR occurs when the artifacts are larger than the breathing signal, for example in episodes of movement without breathing. To avoid the cancellation of the breathing signal when the SAR is high, we introduced a limitation in the adaptive filter gain.

The nonstationary characteristics of these signals, especially for motion artifacts, are a major problem to obtain a fast and accurate

response in the adaptive filter. Further experiments with short time movements and position changes must be done to optimize the filter coefficients.

Cardiac artifact seems a feasible artifact to be reduced using this technique, but measurements in neonates are necessary to know the frequency characteristics of ventilation and artifacts in this population.

ACKNOWLEDGMENT

The authors would like to thank D. Beams for designing the impedance plethysmograph and W. Tompkins for his scientific contributions.

REFERENCES

[1] "Apnea monitoring by means of thoracic impedance pneumography," *AAMI*, Assoc. Advancement of Med. Instrumentation, Arlington, VA, TIR 4-1989, 1989.

[2] A. F. Pacela, "Impedance pneumography—A survey of instrumentation techniques," *Med. Biol. Eng.*, vol. 4, pp. 1–15, 1966.

[3] Consensus statement, "National Institutes of Health consensus development conference on infantile apnea and home monitoring," *Pediatrics*, vol. 79, pp. 292–299, 1987.

[4] T. M. Baird and M. R. Neuman, "Effect of infant position on breath amplitude measured by transthoracic impedance and strain gauges," *Pediatric Pulmonology*, vol. 10, pp. 52–56, 1991.

[5] D. Warburton, A. R. Stark, and H. W. Taeusch, "Apnea monitor failure in infants with upper airway obstruction," *Pediatrics*, vol. 60, pp. 742–744, 1977.

[6] A. V. Sahakian, W. J. Tompkins, and J. G. Webster, "Electrode motion artifacts in electrical impedance pneumography," *IEEE Trans. Biomed. Eng.*, vol. BME-32, pp. 448–451, 1985.

[7] S. Luo, V. X. Afonso, J. G. Webster, and W. J. Tompkins, "The electrode system in impedance-based ventilation measurement," *IEEE Trans. Biomed. Eng.*, vol. 39, pp. 1130–1141, 1992.

[8] K. P. Cohen, S. L. Luo, G. J. Gruber, B. Sheers, J. G. Webster, and W. J. Tompkins, "Accuracy and correlation of abdomen and ribcage impedance and inductance-based ventilation sensors during breathing and motion," submitted.

[9] K. A. East, T. D. East, V. J. Mathews, and B. T. Waterfall, "Computerized artifact detection for ventilatory inductance plethysmographic apnea monitors," *J. Clin. Monit.*, vol. 5, pp. 170–176, 1989.

[10] J. Rosell, J. Colominas, P. Riu, R. Pallás-Areny, and J. G. Webster, "Skin impedance from 1 Hz–1 MHz," *IEEE Trans. Biomed. Eng.*, vol. BME-35, pp. 649–651, 1988.

[11] J. Rosell and J. G. Webster, "Signal-to-motion artifact ratio versus frequency for impedance pneumography," *IEEE Trans. Biomed. Eng.*, vol. 42, pp. 321–323, Mar. 1995.

[12] B. Widrow, J. R. Glover, J. M. McCool, J. Kaunitz, C. S. Williams, R. H. Hearn, J. R. Zeidler, E. Dong, and R. Goodlin, "Adaptive noise cancelling: Principles and applications," *Proc. IEEE*, vol. 63, pp. 1692–1716, 1975.

[13] S. S. Haykin, *Adaptive Filter Theory*. Englewood Cliffs, NJ: Prentice-Hall, 1986.

[14] U.S. Dep. Health Human Services, Public Health Service, "Infantile apnea and home monitoring," Nat. Inst. Health, NIH Publ. 87-2905, 1987.

Adaptive Filtering of the Electromyographic Signal for Prosthetic Control and Force Estimation

Euljoon Park and Sanford G. Meek

***Abstract*—An adaptive time constant filter is derived for electromyographic (EMG) signal processing in prosthetic control applications. The analysis indicates that the mean-squared estimation error can be reduced by varying the time constant of the filter as a function of the signal and its derivative. Results of several experiments indicated this filter provides faster response and smaller estimation error than several previously available filters.**

I. INTRODUCTION

The cutaneously measured EMG signal that arises as a byproduct of muscular contraction has been widely used for the control of prostheses [1]–[4]. Typically, three stages of processing must be performed in order to extract a usable proportional control signal [5]–[8]: 1) band-pass filtering to eliminate extraneous noises, 2) rectification to generate a nonzero mean signal, and 3) low-pass filtering to smooth the signals.

The EMG signal appears as a zero mean, amplitude modulated (AM) voltage, with the muscle force (or command) information modulating a higher frequency carrier-like random noise signal. Unlike a typical AM broadcast system where the spectra of the signal and carrier (noise) are widely separated, the noise spectrum of the rectified EMG overlaps that of the command signal and has a wider power spectrum. Furthermore, we cannot assign a stationary spectral model to the command signal. The muscle force can either be rapidly changing, or relatively constant. The typical bandwidth of force signal is under 3 Hz [5]. The overlapped spectra and the nonstationarity of the command signals pose difficulties with the processing of EMG signals. In order to provide sufficient noise rejection during slow motions as well as quick response to rapid commands, the filter must be able to adapt its bandwidth to the specific signal [5], [8]–[11].

Kreifeldt [2] found that a time averaging filter, for similar rise times, gave a 3–5-dB improvement in signal-to-noise ratio (SNR) over either a first-order filter or a third-order Butterworth filter. Meek *et al.* [12] compared the performance of linear, averaging, and the adaptive time constant filter which is explained later in this section, and reported that the SNR of the adaptive time constant filter was 20% higher than the ratio of a linear filter and 12% higher than that of an averaging filter with the same rise time. Kreidfeldt and Yao [13] evaluated several demodulators by simulation and concluded that root law processors, followed by power law processors, gave higher SNR outputs than conventional full wave rectification. These results are, however, valid in static conditions only [5], [8] and vary with the spectral composition of the EMG signal model. Kaiser *et al.* [14] determined that low frequency modulation of signals by noise could be minimized by distributing noise evenly over a spectrum via a prewhitening filter prior to demodulation. Fullmer [5] reported that the effect of prewhitening on the adaptive time constant filter is not

Manuscript received January 19, 1993; revised April 11, 1995. This work was supported by Biomedical Research Support Grant RR07092-22 from the National Institutes of Health.

E. Park is with Pacesetter, Inc., a St. Jude Medical Company, Sylmar, CA 91392-9221 USA.

S. G. Meek is with the Center for Engineering Design, Department of Mechanical Engineering, University of Utah, Salt Lake City, UT 84112 USA.

IEEE Log Number 9414170.